JOURNAL OF MATERIALS SCIENCE 31 (1996) 713–720

Preparation of BN films by r.f. thermal plasma chemical vapour deposition

S. MATSUMOTO
National Institute for Research in Inorganic Materials, 1-1 Namiki, Tsukuba-shi 305, Japan
N. NISHIDA*, K. AKASHI
Department of Industrial and Engineering Chemistry, Faculty of Science and Technology, Science University of Tokyo, 2641 Yamasaki, Noda-shi 278, Japan
K. SUGAI
Nachi-Fujikoshi Corp., 20 Ishigame, Toyama-shi 930, Japan

Boron nitride films were prepared at 1 atm by r.f. thermal plasma chemical vapour deposition from the gas systems of Ar–BF_3–N_2 (or NH_3, NF_3)–H_2, Ar–BCl_3–N_2 (or NH_3, NF_3)–H_2, and Ar–B_2H_6–N_2 (or NH_3)–H_2. The appearance and the deposition rate of the films changed drastically with the composition of the feed gas. Only from the Ar–BF_3–N_2(–NF_3) gas, were transparent and smooth films obtained, while from other gas systems, white flaky or powder-like deposits formed. The structure of these films was basically sp^2-bonded turbostratic BN, and the formation of cubic BN was not confirmed.

1. Introduction

Preparation of cBN from low-pressure gas phase has been tried mainly by two methods, namely physical vapour deposition (PVD), which utilizes bombardment of energetic particles on the substrate [1–6], and chemical vapour deposition (CVD) [7, 8]. Both methods have had partial success, i.e. BN films with small crystallites which show an infrared absorption in the range of 1020 [9]–1110 [10] cm^{-1} and electron diffraction corresponding to cBN. The infrared absorption which was attributed to cBN has been reported to change its peak position within the above region according to the synthesis conditions due to residual stresses and crystal imperfections in the film. This region (1020–1110 cm^{-1}) is termed region A in this paper. In these methods, relatively low gas pressures were used for synthesis, i.e. 10^{-5}–10^{-3} torr (1 torr = 133.322 Pa) in PVD and 10^{-1}–100 torr in CVD.

In this paper, we report the results of an attempt to prepare cBN at atmospheric pressure by r.f. thermal plasma CVD using various feed-gas systems, especially fluorine-containing gases; fluorine was expected to react with BN and to play such a role as atomic hydrogen does in diamond synthesis, as suggested by the large formation energy of BF_3 and the availability NF_3 gas. The formation of cBN by using BF_3 in electron cyclotron resonance (ECR) [10] and parallel plate [11] plasma CVD has been reported so far. BCl_3 and B_2H_6 are also used instead of BF_3. The details of these results will be described.

2. Experimental procedure

The apparatus used is almost the same as used previously [12]. The torch, which is shown schematically in Fig. 1, is made of a double-walled quartz tube and a metal nozzle through which three kinds of gas were injected, i.e. tangential sheath, axial plasma and axial central gas (carrier and reactant gas). This torch was set on a metal chamber which was evacuated by an oil-rotary pump and a mechanical booster pump. The background pressure before the deposition was 1×10^{-2} torr. The gas systems used were mainly BF_3–N_2–Ar, BF_3–NF_3–Ar, BF_3–N_2–NF_3–Ar, and those including hydrogen as NH_3 and/or H_2. As an example, experimental conditions for the BF_3–N_2–NF_3–Ar system are summarized in Table I. For comparison, B_2H_6 or BCl_3 was also used instead of BF_3. BF_3, B_2H_6, BCl_3, and NF_3 were purchased as diluted by argon: the concentrations were 3.76%, 4.68%, 4.9%, and 10.5%, respectively. BF_3(B_2H_6, BCl_3) was introduced with a carrier argon gas, while hydrogen and ammonia were with a sheath argon, and nitrogen and NF_3 were introduced with a carrier or with a sheath gas. The deposition pressure used was 1 atm. Molybdenum plates of 20 mm diameter and 1 mm thickness, or a silicon (100) wafer of 14 mm × 14 mm × 0.5 mm was used as a substrate. The former was scratched on a glass plate with diamond paste and the latter was treated ultrasonically with diamond powders in ethanol. The particle size of both diamonds was 5–10 μm. The substrate was set on a water-cooled substrate holder and heated in the

* *Present address*: Iron and Steel Research Laboratory, Sumitomo Metal Industries Ltd, 1–8 Fusocho, Amagasaki-shi 660, Japan.

0022–2461

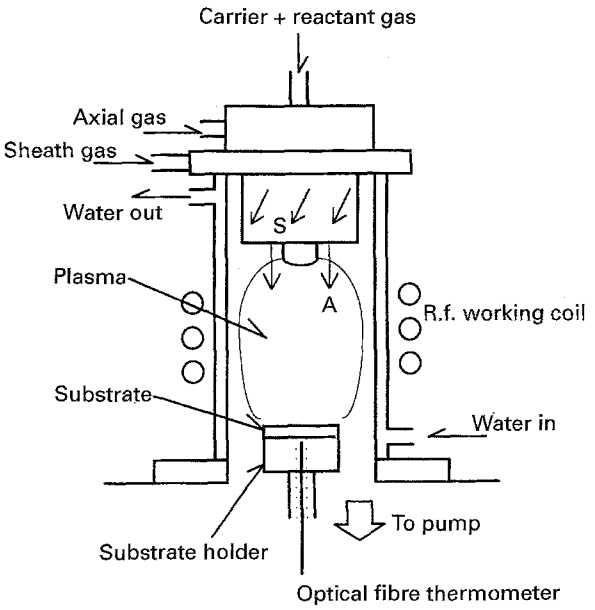

Figure 1 Schematic illustration of the r.f. induction plasma torch used for the deposition.

TABLE I Deposition conditions for the BF_3 system

Gas flow rate	
Ar sheath	15–25 l min^{-1}
Axial	1 l min^{-1}
Carrier	0.4–1 l min^{-1}
H_2	5–1000 ml min^{-1}
BF_3	2.5–25 ml min^{-1}
N_2	5–1000 ml min^{-1}
NH_3	5–20 ml min^{-1}
NF_3	1–60 ml min^{-1}
Pressure	760, 50 torr
Substrate temperature	430–1100 °C
Plate power	10–45 kW

plasma without any external heating. The substrate temperature was measured from the back side by an optical pyrometer using a sapphire rod sensor and a glass fibre transmitting system (Accufiber Model 100). The deposition time was 5 or 10 min for each run.

Prepared films were observed by secondary electron microscopy (SEM, Akashi-Topcon ISI-DS130) and characterized by X-ray diffraction (XRD, Rigaku RINT 2500), Fourier transform–infrared (FT–IR) spectroscopy (BIO-RAD FTS-65), electron spectroscopy (XPS, Vacuum Generators MICRO LAB 320-D) and electron probe microanalysis (EPMA, Shimadzu EMX SM7). In infrared absorption measurement, the deposits on molybdenum plates were scratched off by rubbing with KBr powders and measured by diffuse reflectance spectroscopy (IRDRS) and the films on silicon wafers were measured by transmission through the substrates. XPS and EPMA measurements were done without any surface treatment.

3. Results

The appearance of the deposits obtained in all the experiments is summarized in Table II. The structure of all the deposits is basically sp^2-bonded turbostratic BN (tBN). As noted in the table, some of the deposits showed an infrared absorption(s) in region A. However, some of them are due to the presence of SiO_2 and others are not yet assigned. The details of these results will be described below.

3.1. B–N–F–Ar system

In this system, the deposition behaviour is classified into three cases according to the gas composition and substrate temperature: (a) deposition of smooth and transparent films, (b) deposition of smooth but brown films, (c) no deposition or etching of the substrate. Fig. 2 summarizes the relations between the appearances of the deposits and the composition of the feed gas.

3.1.1. BF_3–N_2–Ar system

In this system, transparent and smooth films were obtained in a wide range of substrate temperature, i.e. 500–1100 °C, if the ratio of N_2 to BF_3 was higher than about 2. Film thickness was measured only for a few samples. An example of the deposition rate was about 1 μm min^{-1} at 700 °C (for the film shown later in Fig. 5b). A typical SEM image of these films is shown

TABLE II Summary of the appearances of the deposits

	Gas system[a]	Appearance of the deposit	Corresponding SEM image
1. (a)	$BF_3 + N_2$	Transparent smooth film[b]	Fig. 3
	$BF_3 + NF_3$	Transparent or brown film[b]	
	$BF_3 + NF_3 + N_2$	Transparent or brown film[b]	
(b)	$BF_3 + N_2 + H_2$	White film[c]	
	$BF_3 + NH_3(+ H_2)$	White film or flaky deposits[c]	Fig. 8 (the former)
2.	$BCl_3 + N_2$	White powder-like deposits	Fig. 11
	$BCl_3 + NH_3 + H_2$	White flaky deposits	
	$BCl_3 + NF_3$	Grey, matt deposits (Mo_2N + MoN)	
3.	$B_2H_6 + N_2$	White powder-like deposits	
	$B_2H_6 + NH_3(+ H_2)$	White flaky deposits[c]	Fig. 12

[a] All the gas systems include argon.
[b] Usually show an infrared absorption(s) in region A(1020–1110 cm^{-1}).
[c] Some of the specimens show an infrared absorption(s) in region A.

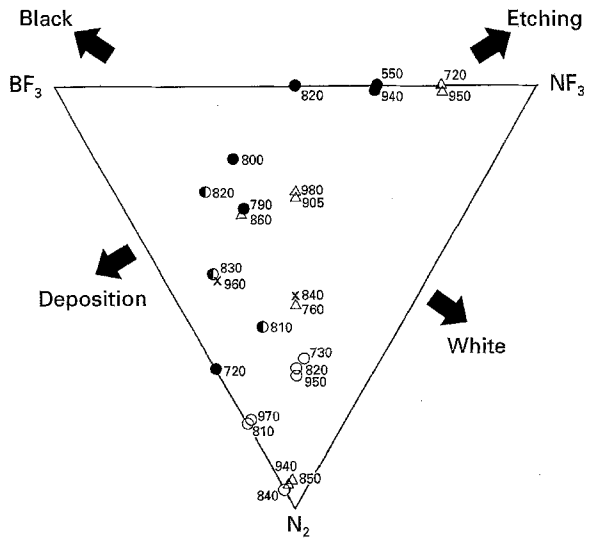

Figure 2 Summary of the appearance of the depositions in a B–N–F diagram by using various compositions of the feed gas of $BF_3 + N_2 + NF_3$. The substrate temperatures during deposition are shown. (○, ●) Deposition at high rate, (△, ▲) slow deposition, (×) no deposition or etching of the substrate, (●, ▲) brown deposits, (○, △) transparent deposits, (◐) partly brown deposits.

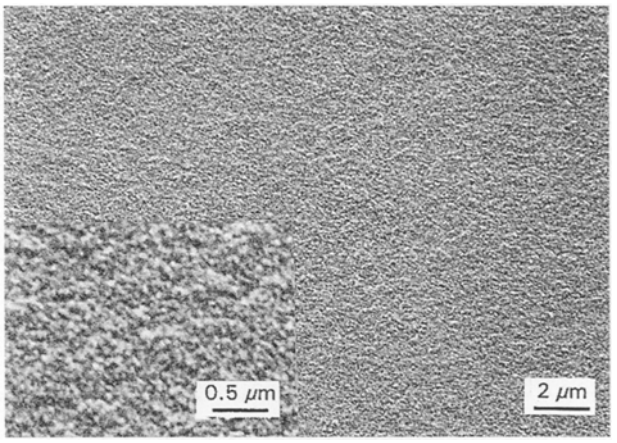

Figure 3 SEM image of the film obtained by feeding 5 standard $cm^3\,min^{-1}$ BF_3 and 100 standard $cm^3\,min^{-1}$ N_2 at 995 °C substrate temperature.

in Fig. 3, which reveals that the surface is fairly smooth and the grain size of the film is ~30–50 nm.

Fig. 4 shows a glancing-angle XRD pattern of the film deposited from this gas system on a silicon substrate. A broad peak at $\sim 2\theta = 25.5°$ can be attributed to the 0 0 2 reflection of hBN. The shift of the hBN peak ($2\theta = 26.8°$) to the lower angle indicates that stacking of the layers is not in good order, but has some expansion. The second strongest reflection is seen with its peak position at $2\theta = 42.5°$. This value is in between those of 1 0 0 and 1 0 1 reflections of hBN ($2\theta = 41.6°$ and 43.9°, respectively) and wBN and cBN also have reflections at around this angle as indicated in Fig. 4. Although the possibility of the presence of wBN and cBN in this film cannot be excluded completely, it is most probable that this broad peak is the 10 reflection of turbostratic BN (tBN) which appears owing to irregular stacking of hexagonal network layers of boron and nitrogen in the *c* crystallographic axis [13]. These results suggest that the structure of the films from BF_3–N_2 gas is mainly tBN. In addition to these broad peaks, the formation of Mo_2B and MoB was observed on molybdenum substrates when the deposition temperature was higher than ~ 1000 °C, and Mo_2N was observed when the temperature was lower. The formation of crystalline SiB_x ($x = 4$, 6) on silicon substrates (even at $T_s = 953$ °C) was not detected by XRD.

Examples of infrared spectra of the films on molybdenum and on silicon are shown in Fig. 5. IRDRS are not transformed into the Kubelka-Munk form in this report. Major absorptions are at ~1400 and 800 cm^{-1}, which can be assigned to in-plane and out-of-plane TO modes of hBN, respectively. In addition to these peaks, a small absorption is seen at ~1100 cm^{-1} in Fig. 5a, and a shoulder absorption at 1080 cm^{-1} in Fig. 5b. These wave numbers are within region A of cBN. However, it cannot be concluded to be from cBN, because we could not find a pattern of cBN in the electron diffraction of these films from BF_3–N_2 gas. There are many other candidates for these absorptions, as will be described below (Section 4). The film on silicon shows additional absorptions at 3200–3600 cm^{-1}. These absorptions appeared even when the substrate temperature was as high as 953 °C. Incorporation of NH_x is the most probable origin of these absorptions, but the coexistence of –OH structures cannot be excluded, as will also be discussed in Section 4.

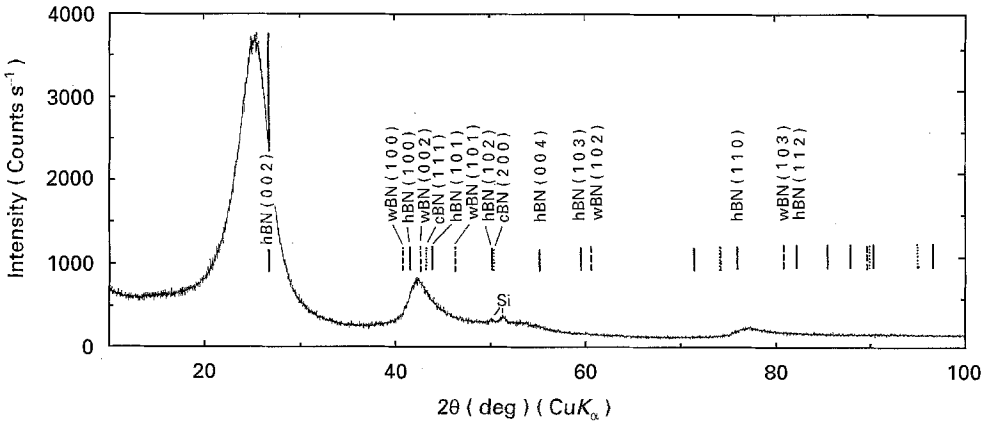

Figure 4 Glancing-angle X-ray diffraction profile of the film from BF_3–N_2–Ar gas (the same specimen as in Fig. 5b). Incident angle: 0.5°.

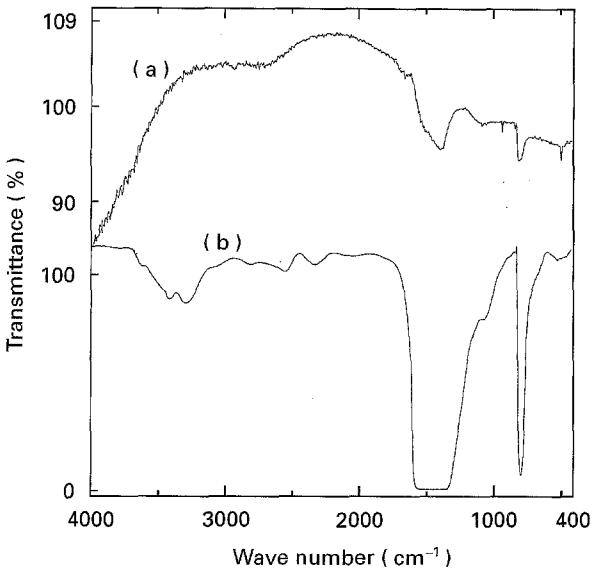

Figure 5 (a) Infrared diffuse reflectance spectrum (IRDRS) of the film deposited on molybdenum by feeding 5 standard cm^3 min^{-1} BF_3 and 100 standard cm^3 min^{-1} N_2 at 840 °C. (b) Infrared transmission spectrum of the film deposited on silicon by feeding 5 standard cm^3 min^{-1} BF_3 and 700 standard cm^3 min^{-1} N_2 at 690 °C.

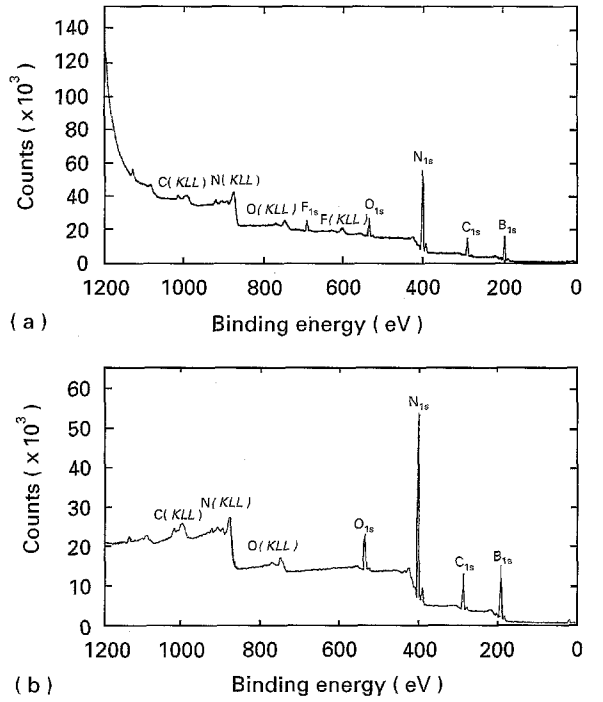

Figure 6 (a) XPS spectrum of the film obtained on silicon at 950 °C from 5 standard cm^3 min^{-1} BF_3 + 200 standard cm^3 min^{-1} N_2 + 27 standard l min^{-1} Ar gas. (b) XPS spectrum of a pyrolytic boron nitride plate (Shin-etu Kagaku Co.).

The XPS spectrum of the film on silicon is shown in Fig. 6 together with that of pyrolitic BN (pBN, Shin-etsu Kagaku Co.). B_{1s} and N_{1s} peaks are seen in both spectra and C_{1s} and O_{1s} peaks are also seen, which have been popularly observed in BN films from the gas phase (e.g. [14]). The intensities of the B_{1s} and N_{1s} peaks relative to those of C_{1s} and O_{1s} are very close for the two samples, and the B_{1s}/N_{1s} ratios are also similar (0.32 for the film in Fig. 6a and 0.28 for the pBN).

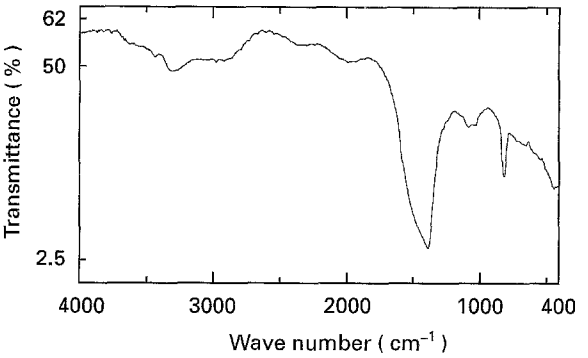

Figure 7 Infrared spectra of the films obtained on silicon, from 5 standard cm^3 min^{-1} BF_3 + 10 standard cm^3 min^{-1} NF_3 + 27 standard l min^{-1} Ar at 940 °C.

3.1.2. BF_3–NF_3–Ar system

In this system, the appearance of the deposits changed in three ways according to the NF_3/BF_3 ratio. When the NF_3/BF_3 ratio was lower than ~ 2, brown deposits were obtained on molybdenum substrates, and when the ratio was higher than ~ 6, the substrate was partly etched and partly covered with dark brown deposits. Infrared spectroscopy suggested the deposition of boron (amorphous) for the former and XRD revealed the formation of Mo_2N for the latter. When the ratio was between ~ 2 and ~ 4, the films showed absorptions at ~ 1380, 800 cm^{-1} and region A in the infrared spectra, and B_{1s} and N_{1s} peaks in XPS. However, O_{1s} (and F_{1s}) peaks were higher than those in the films from the BF_3–N_2 system. The brown colour is probably due to excess boron in the films. The deposition rate was lower than the BF_3–N_2–Ar system.

Examples of infrared spectra are shown in Fig. 7 for the films prepared on silicon under the conditions of $NF_3/BF_3 = 2$. As compared with the deposits from the BF_3–N_2 system, absorptions due to hBN are weak and the absorptions in region A, whose peaks are at 1081 and 1017 cm^{-1}, are well separated from the peak of hBN. However, an absorption at ~ 450 cm^{-1} suggests the possibility of the incorporation of some silicon oxide, which also shows an absorption(s) in region A [15]. Oxygen and fluorine peaks in the XPS spectra were stronger than those of the film from BF_3–N_2 gas. This supports the idea that at least one of the infrared absorption(s) in region A is due to the presence of SiO_2. An increased amount of fluorine in the gas phase may promote the formation of SiO_2 owing to the oxidizing power of fluorine, or it may be only because slow deposition of BN makes the presence of SiO_2 clear. Because these IR peaks are all very weak and the amount of the deposits is very small, the identification of their structure was not possible.

3.1.3. BF_3–N_2–NF_3–Ar system

As described above, in the BF_3–N_2 system, transparent tBN deposited with a high growth rate when the ratio N_2/BF_3 was high, and excess boron was included when the ratio was low (below ~ 2). On the contrary, in the BF_3–NF_3 system, when the ratio NF_3/BF_3 was high, the substrate was etched and BN

was not obtained and when the ratio was low, the deposition rate of tBN was low and excess boron was included. Therefore, in this BF_3–N_2–NF_3 system, we expected to obtain colourless BN with a slow deposition rate for selective deposition of cBN. According to the composition of the feed gas, the deposition rate and tendency to include excess boron changed as illustrated qualitatively in Fig. 2. This means that we could control the etching effect of fluorine by changing the N_2/NF_3 ratio. For example, a transparent flat film was obtained by feeding 10 standard $cm^3\ min^{-1}$ BF_3, 5 standard $cm^3\ min^{-1}$ NF_3 and 7 standard $cm^3\ min^{-1}$ N_2. In these flow rates, without either NF_3 or N_2, a dark brown film was deposited. Although the above film showed an infrared absorption at 1088 cm^{-1}, it seemed also to be due to the incorporation of SiO_2 as in the BF_3–NF_3 system.

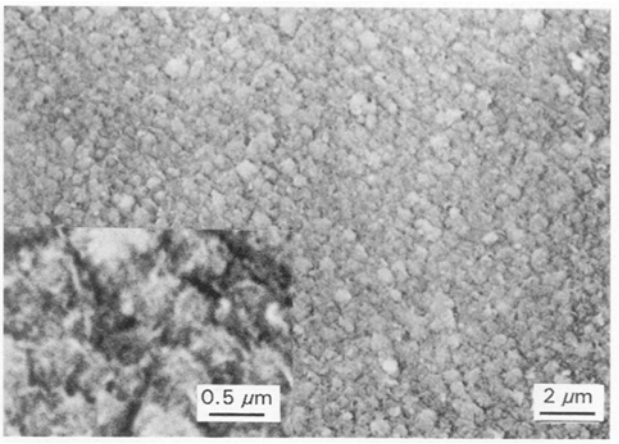

Figure 8 SEM image of the film from 5 standard $cm^3\,min^{-1}$ BF_3 + 10 standard $cm^3\,min^{-1}$ NH_3 + 100 standard $cm^3\,min^{-1}$ H_2 + 27 standard $l\,min^{-1}$ Ar on silicon at 810 °C.

3.2. B–N–F–H–Ar system

Because the compositions in this system are very complicated, a qualitative description on the effects of hydrogen which was added as NH_3 or H_2 will be noted. Not so much NH_3 was added, i.e. < 10 standard $cm^3\ min^{-1}$ ($NH_3/BF_3 < 2$), while up to 1 standard $l\ min^{-1}$ H_2 was added at maximum.

When only NH_3 was used as a source for nitrogen or a small amount ($1 < H/F < 20$) of hydrogen was added to BF_3–N_2, surface brightness decreased even when transparent, and the film became white by increasing the amount of hydrogen further. As an example of the former, Fig. 8 shows a scanning electron micrograph of the film deposited by using 5 standard $cm^3\ min^{-1}$ BF_3, 10 standard $cm^3\ min^{-1}$ NH_3 and 100 standard $cm^3\ min^{-1}$ H_2 at 800 °C. The grain size appears to be ~500 nm at low magnification, which is about ten times larger than that of the film obtained in BF_3–N_2 gas (Fig. 3), but a flake-like structure is seen at high magnification. The flaky structure is very common in the white films obtained by using BCl_3 or B_2H_6 gas instead of BF_3 (see Fig. 12 below).

Features of IR absorption spectra in region A did not change so much when the amount of hydrogen added was small, i.e. an absorption(s) in region A appeared as a shoulder or as small peaks. For example, a spectrum of the film in Fig. 8 is shown in Fig. 9a. The infrared spectrum of the film obtained by adding 10 standard $cm^3\ min^{-1}$ NF_3 was also similar to this. A strong and broad absorption whose peak is at ~3260 cm^{-1} is seen in Fig. 9a. A similar absorption was observed in Fig. 5b. When the amount of hydrogen was increased up to 1 standard 1 min^{-1}, the absorption in region A was very weak and that at ~3260 cm^{-1} disappeared (Fig. 9b). Fig. 10 shows the XRD pattern of this film. The respective shifts of the 0 0 2 and 1 0 peaks to higher ($2\theta = 25.8°$) and lower ($2\theta = 42.1°$) angles and the separation of the 1 1 peak to 1 1 0 and 1 1 2 suggest that stacking of BN layers of this tBN is more hBN-like than that of the film from BF_3–N_2 gas (Fig. 3).

The deposition rate apparently increased and the brown colour of the film decreased slightly when hydrogen was added to the BF_3–NF_3 system, where the etching effect of fluorine is large. These effects of hydrogen addition are probably due to the formation of HF, which releases boron from BF_3 to deposit BN, as will be discussed in Section 4.

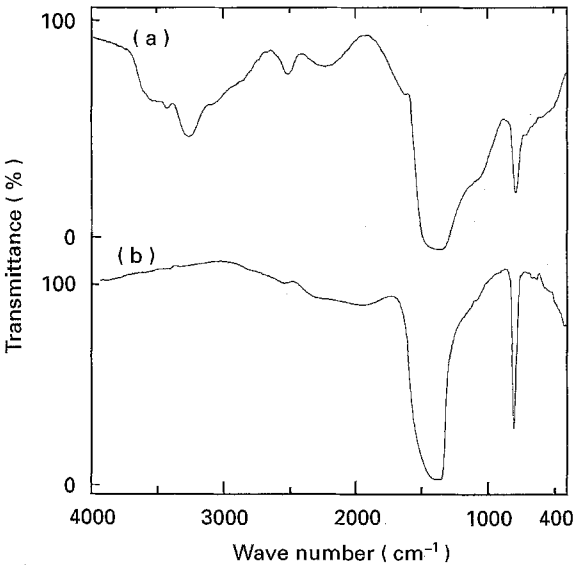

Figure 9 Infrared spectra of the films from BF_3–NH_3–H_2–Ar gas. (a) The same specimen as in Fig. 8. (b) Specimen obtained from 5 standard $cm^3\,min^{-1}$ BF_3 + 10 standard $cm^3\,min^{-1}$ NH_3 + 1 standard $l\,min^{-1}$ H_2 + 27 standard $l\,min^{-1}$ Ar on silicon at 850 °C.

3.3. BCl_3–N_2–(H_2)–Ar, BCl_3–NH_3–(H_2)–Ar, BCl_3–NF_3–Ar system

From the first and the second gas systems of the above, white deposits were obtained, by using either N_2 or NH_3. However, the appearance of the deposits from gas systems with H_2 is a little different to those from systems without H_2. The deposits from the former were flaky while from the latter they were powder-like. These deposits did not show infrared absorption in region A. An example of an SEM image of the powder-like deposits on molybdenum from a BCl_3–N_2 gas is shown in Fig. 11. From the BCl_3–NF_3–Ar gas system, matt, grey deposits were obtained on molybdenum, which were

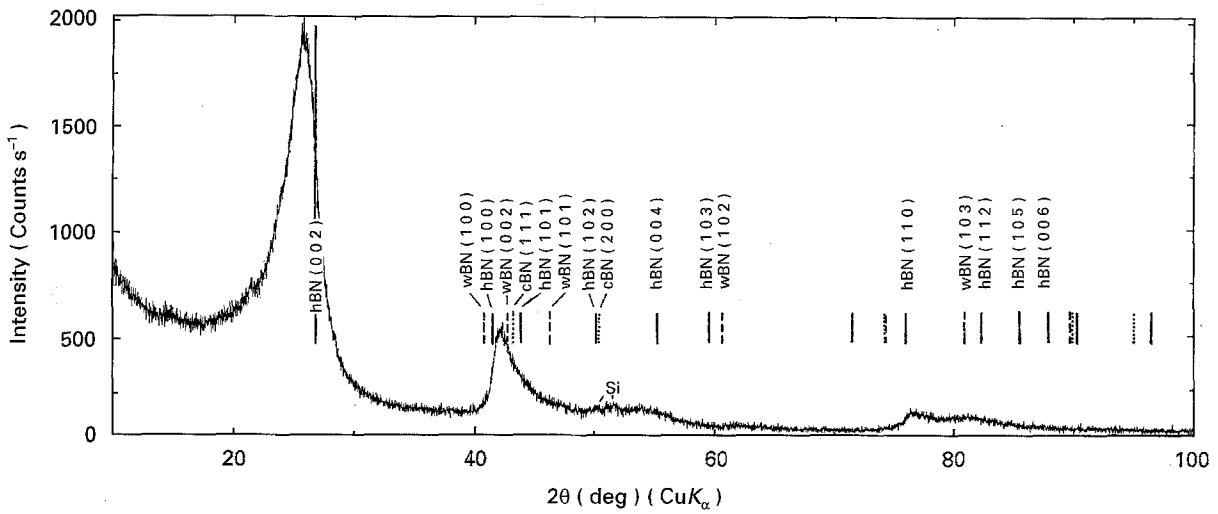

Figure 10 Glancing-angle X-ray diffraction profile of the film from BF_3–NH_3–H_2–Ar gas (the same specimen as in Fig. 9b).

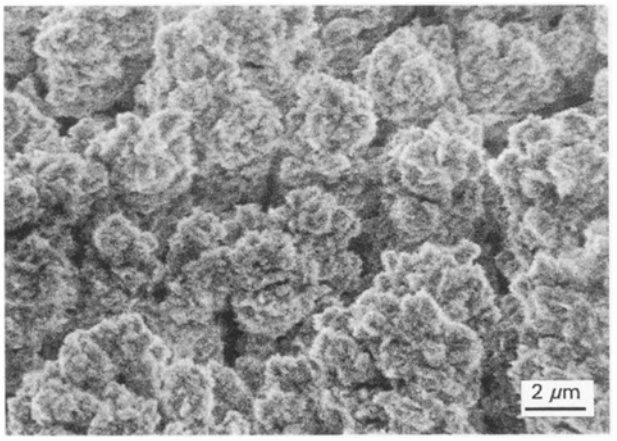

Figure 11 SEM image of the deposit from 2.5 standard $cm^3\,min^{-1}$ BCl_3 + 1 standard $l\,min^{-1}$ N_2 + 27 standard $l\,min^{-1}$ Ar at 760 °C.

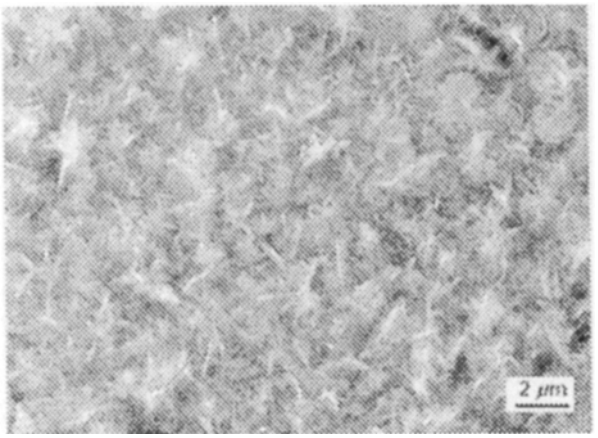

Figure 12 SEM image of the film obtained from 2.5 standard $cm^3\,min^{-1}$ B_2H_6 + 10 standard $cm^3\,min^{-1}$ NH_3 + 1 standard $l\,min^{-1}$ H_2 + 27 standard $l\,min^{-1}$ Ar at 845 °C on molybdenum.

identified to be a mixture of Mo_2N and MoN by XRD.

3.4. B_2H_6–N_2(–H_2)–Ar, B_2H_6–NH_3(–H_2)–Ar system

In this system also, white deposits were obtained. As in Section 3.3, when the amount of hydrogen in the gas system was small, i.e. from B_2H_6–N_2–Ar gas, powder-like deposits were obtained, while in other cases (by using NH_3 or a large amount of hydrogen) flaky deposits were formed. A typical scanning electron micrograph of the latter is shown in Fig. 12. However, IRDRS of the films obtained on molybdenum by using NH_3 often showed an infrared absorption in region A, without accompanying an absorption at ~450 cm^{-1}, where silicon oxides have an absorption, but it was weak, as was usual in the BF_3–N_2(–H_2)–Ar system described in Section 3.1. The results of this system will be summarized in detail in another paper.

4. Discussion

From the results of XRD and infrared absorption measurements, it can be concluded that tBN is obtained in all the gas systems used if the gas composition is appropriate. If the amount of hydrogen used is small, BN films from the B–N–F–H–Ar system usually show an infrared absorption(s) in region A (1020–1110 cm^{-1}) where the absorption of cBN appears. The following origins of these peaks can be proposed, in addition to cBN. (1) Incorporation of SiO_2. In this case, another absorption is observed in the range 464–450 cm^{-1}. This seems to occur when the amount of fluorine in the gas system increases. (2) Some structure related to metal borides. Infrared spectra of many borides show an absorption at ~ 1080 cm^{-1} [15]. No survey has been made to assign this boride's peak, but there is a possibility that the peaks at region A are also related to the presence of silicon borides or molybdenum borides. (3) Some metal fluoroborates also have an absorption in this range [15]. (4) The presence of boron oxides or boric acids. (5) Some complexes or compounds from ammonia and boron fluoride.

Absorptions at 3200–3700 cm^{-1} suggest the presence of NH_x and/or OH structures. Possible candidates for these are: (1) residual NH_x in the BN films, (2) hydrated boron oxides or boric acids, (3) hydrated silicon oxides or silicic acids, (4) some fluoroborates and their water crystallization, (5) some complexes or

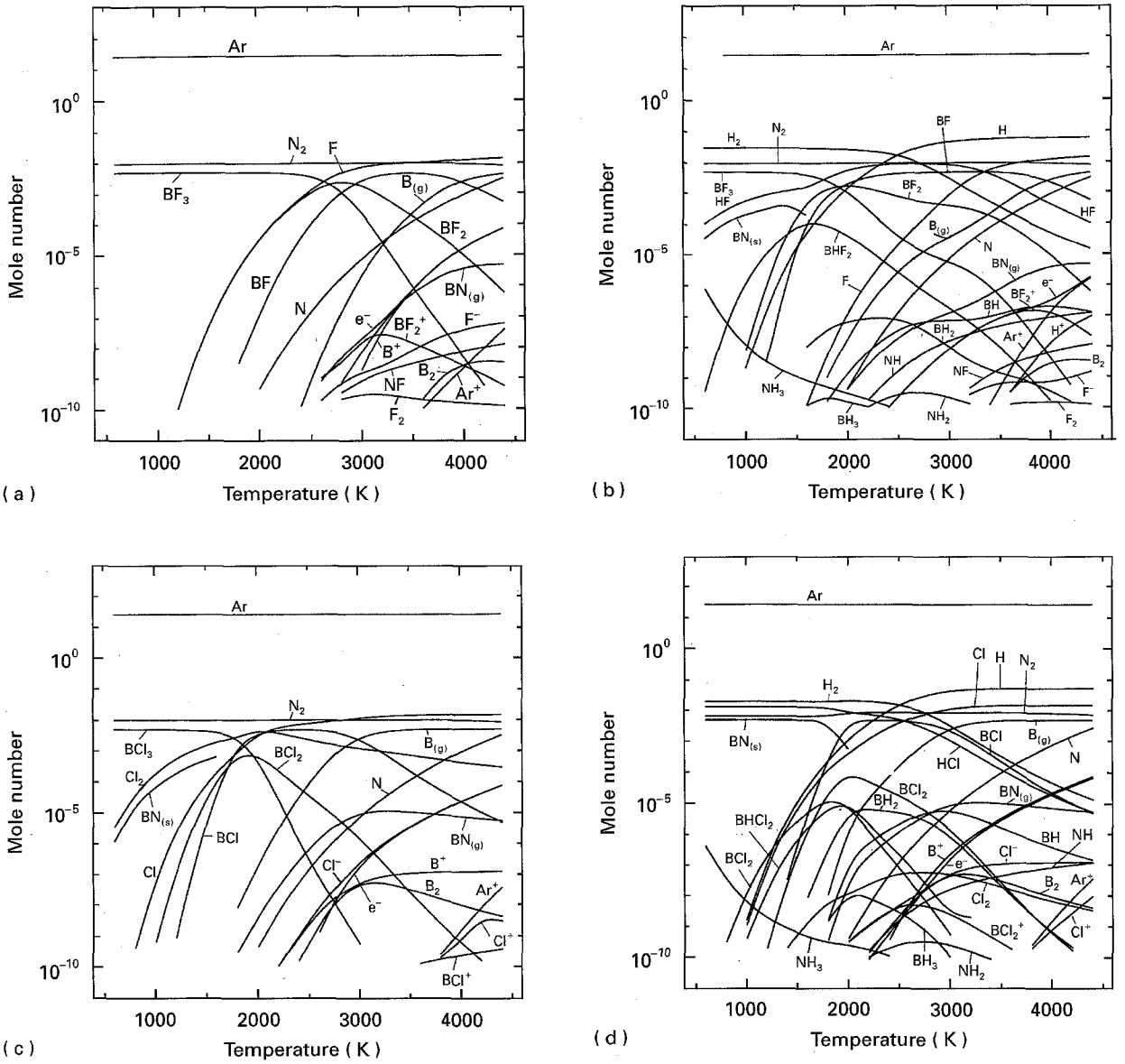

Figure 13 Equilibrium compositions at 1 atm calculated by the VCS method for (a) BF_3–N_2–Ar, (b) BF_3–NH_3–Ar, (c) BCl_3–N_2–Ar, (d) BCl_3–NH_3–Ar, (e) B_2H_6–N_2–Ar systems. The verticals show mole numbers produced per minute by feeding 5 standard $cm^3\,min^{-1}$ BF_3 (or BCl_3, $1/2B_2H_6$) + 10 standard $cm^3\,min^{-1}$ N_2(2 NH_3) + 27 standard $l\,min^{-1}$ Ar.

compounds from ammonia and boron fluoride. Many of these compounds have an infrared absorption in region A. Thus, the formation of cBN was not confirmed in the deposits from any gas system used by this thermal plasma CVD method. To make the assignment of the IR absorptions in region A clearer, deposition experiments, using an apparatus with less leakage or contamination, are necessary.

As described above, only from the BF_3–N_2(–NF_3) system, were transparent and smooth films obtained. When a large amount of hydrogen was added to this system, or B_2H_6 or BCl_3 was used instead of BF_3, white flaky or powder-like deposits were obtained. It is natural that flaky or powder-like products are deposited at 1 atm, because molecular collision in the gas phase is very frequent. The reason why only transparent and smooth films are deposited in BF_3–N_2–(NF_3) system is speculated as follows by considering the results of the calculation of the equilibrium composition of the systems used. The calculation was done by using the VCS method [16] and JANAF thermochemical data [17]. Fig. 13 shows the

results for BF_3–N_2, BF_3–NH_3, BCl_3–N_2, BCl_3–NH_3, and B_2H_6–N_2 systems. We can understand from these figures that only in the BF_3–N_2 system (Fig. 13a), is BF_3 stable up to ~ 2000 K, and solid BN does not appear, while BCl_3 and B_2H_6 decompose partly or almost completely even at low temperatures, forming solid BN (Fig. 13c–e). This means that fluorine has an ability to dissolve solid BN into the gas phase. However, when hydrogen is added to the B–F–N system, HF appears as a stable species and BF_3 partly decomposes at low temperatures, forming solid BN (Fig. 13b). It should be noted here even in thermal plasma processes, thermochemical equilibrium is not achieved completely in the actual experimental apparatus, and this may be the reason why solid BN deposited from the BF_3–N_2 system, even though it does not appear in Fig. 14a. This uniqueness of BF_3–N_2 system seems to be correlated with the reason why smooth and transparent films were obtained from this system only. However, this ability of fluorine to dissolve much BN into the gas phase does not seem to contribute to the selective deposition of cBN.

5. Conclusions

BN films were prepared at 1 atm by r.f. induction thermal plasma CVD on silicon and molybdenum substrates.

1. From $BF_3 + N_2$, $BF_3 + NF_3$, $BF_3 + N_2 + NF_3$ systems, transparent and smooth films were obtained and when much hydrogen was added to this system, white and flaky films were deposited.

2. White powder-like and white flaky deposits were obtained from $BCl_3 + N_2$ and $B_2H_6 + N_2$, and from $BCl_3 + NH_3 + H_2$ and $B_2H_6 + NH_3 + H_2$, respectively.

3. The structure of all the BN films obtained was basically of tBN. Films from $BF_3 + N_2$, $BF_3 + NF_3$, $BF_3 + N_2 + NF_3$ and some of those from $BF_3 + N_2 + H_2$, $BF_3 + NH_3 + H_2$, $B_2H_6 + NH_3 + H_2$ showed an infrared absorption(s) in the range of 1020–1110 cm^{-1}, but some of these are due to silicon oxides, and the formation of cBN was not confirmed.

4. Compared to hydrogen, fluorine suppressed the deposition of solid BN. This fact and conclusions 1 and 2 can be correlated with the results of the calculation of thermochemical equilibrium compositions, but fluorine does not seem to assist the selective deposition of cBN.

Acknowledgements

The authors thank Mr K. Hoshino, Rigaku Denki Co., and Dr M. Mukaida, National Institute of Materials and Chemical Research, for the XRD and ellipsometry measurements, respectively. They also thank Dr M. Ishii, Mr M. Tsutsumi and Mr K. Kosuda for advice and for performing FT–IR, SEM and EPMA measurements, respectively, and Mr Y. Shirakawa, Ms H. Ohashi, and Dr J. Tanaka for the XPS measurements.

References

1. M. SOKOLOWSKI, *J. Crystal Growth* **46** (1979) 136.
2. C. WEISSMANTEL, K. BEWILOGUA, D. DIETRICH, H.-J. ERLER, H.-J. HINNEBERG, S. KLOSE, W. NOWICK and G. REISE, *Thin Solid Films* **72** (1980) 19.
3. M. SATOU and F. FUJIMOTO, *Jpn J. Appl. Phys.* **22** (1983) L171.
4. S. SHANFIELD and R. WOLFSON, *J. Vac. Sci. Technol.* **A1** (1983) 323.
5. K. INAGAWA, K. WATANABE, I. TANAKA, S. SAITOH and A. ITOH, in "Proceedings of the 9th Symposium on Ion Source and Ion-assisted Technology" (ISIAT), edited by T. Takagi (Ion Beam Eng. Exp. Lab., Kyoto University, Kyoto, Japan, 1985) p. 299.
6. A. CHAYAHARA, H. YOKOYAMA, T. IMURA and Y. OSAKA, *Jpn J. Appl. Phys.* **26** (1987) L1435.
7. S. KOMATSU, K. AKASHI and T. YOSHIDA, in "Proceedings of the 7th International Symposium on Plasma Chemistry", Eindhoven, July 1985, edited by C. J. Timmerman (IUPAC Subcommittee of Plasma Chemistry, 1985) p. 142.
8. H. SAITOH, T. ISHIGURO and Y. ICHINOSE, in "Proceedings of the 8th International Symposium on Plasma Chemistry", Tokyo, August 1987, edited by K. Akashi and A. Kimbara (IUPAC Subcommittee of Plasma Chemistry, 1987) 1148.
9. H. SAITOH and W. A. YARBROUGH, *Appl. Phys. Lett.* **88** (1991) 2228.
10. S. Y. SHAPOVAL, V. T. PETRASHOV, O. A. POPOV, A. O WESTNER, M. D. YODAR and C. K. C. LOK, *ibid.* **57** (1990) 1885.
11. M. MENDEZ, S. MUHL, M. FARIAS, G. SOTO and L. COTA-ARAIZA, *Surf. Coat. Technol.* **41** (1991) 422.
12. S. MATSUMOTO, M. HINO and T. KOBAYASHI, *Appl. Phys. Lett.* **51** (1987) 737.
13. J. THOMAS Jr, N. E. WESTON and T. E. O'CONNOR, *J. Am. Chem. Soc.* **24** (1963) 4619.
14. C. GUIMON, D. GONBEAU, G. PFISTER-GUILLOUZO, O. DUGNE, A. GUETTE, R. NASLAIN and M. LAHAYE, *Surf. Interface Anal.* **16** (1990) 440.
15. R. A. NYQUIST and R. O. KAGEL, "Infrared Spectra of Inorganic Compounds" (Academic Press, New York, 1971).
16. W. R. SMITH and R. W. MISSEN, "Chemical Reaction Equilibrium Analysis" (Wiley, New York, 1982).
17. D. STULL and H. PROPHET (project directors), "JANAF Thermochemical Tables", 2nd Edn (American Chemical Society and American Physics Institute for the National Bureau of Standards, the Superintendent of Documents, US Government Print Office, 1972).

Received 9 August 1994
and accepted 22 June 1995